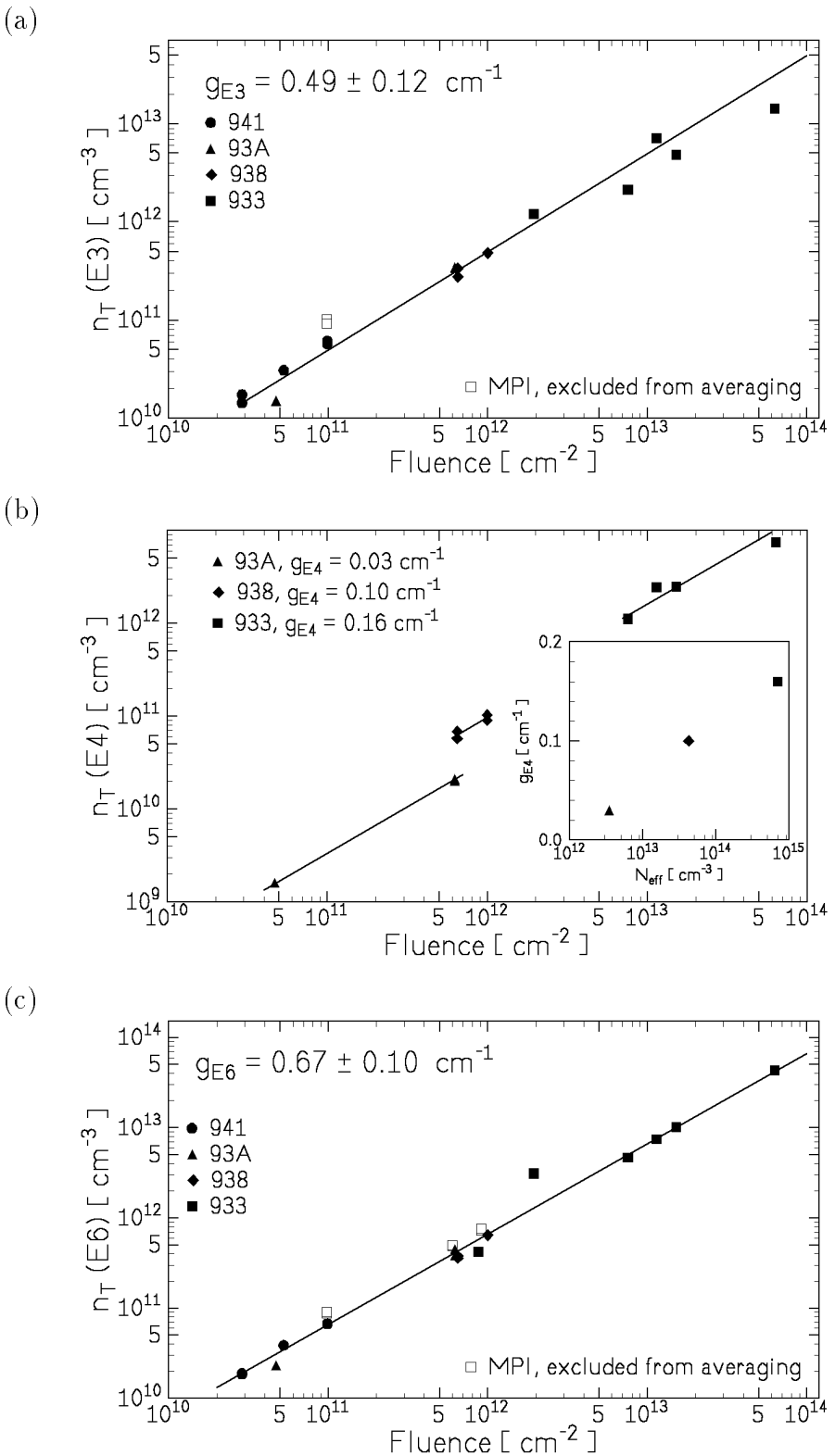

Figure 7.13: Fluence dependence of trap concentration 30 days after irradiation. (a) peak E3, (b) peak E4 and (c) peak E6. Average values were used in the inset of (b) to demonstrate the trend that the generation rate increases with N_{eff} . The p^+-n -samples (MPI) were excluded from the analysis, see text. Note that for all measurements a filling time of t_f = 1 ms was used.

Label	ΔE_C $[eV]$	σ_n $[cm^2]$	g $[cm^{-1}]$	Supposed Identity
E3	0.17	$1{\cdot}10^{-14}$	0.49 ± 0.12	V-O / C_i-C_s
E4	0.25	$5{\cdot}10^{-15}$	0.03 -0.16	V-$V^=$
E6	0.43	10^{-15}	0.67 ± 0.10	

Table 7.5: Generation rates of defects corresponding to peaks E3, E4, and E6, as obtained from different wafers. The p^+-n -samples (MPI) were excluded from the analysis (see text). Note that E4 levels were not completely filled.

As opposed to the generation rate of peak E3, which is expected to be independent of the materials resistivity according to its identification as the V-O complex, the generation rate of the peak E6 had to depend rather sensitively on the resistivity of the material, if peak E6 is correlated to a phosphor related defect.

Assuming that all removed donors are trapped in a V-P complex the generation rate is connected with the donor removal rate by

$$g_{V-P} = N_{D,0} c_C \,, \tag{7.3}$$

if the exponential term is approximated by a Taylor series as possible in case of low fluences. Because c_C is a parameter independent of the initial phosphorus concentration, the generation rate had to grow in proportion to $N_{D,0}$.

Thus the low resistivity material with a high phosphorus concentration should exhibit a much greater generation rate than the material with the low phosphorus concentration, if the E-centre contributed significantly to peak E6.

Deconvoluting the peak as proposed in sec. 7.1.3 the fluence dependence of E6 can be separated into two parts and then the generation rates of both levels, g_{E6a} and g_{E6b} can be determined indiviually. Assuming g_{E6b} to correspond with g_{V-P} the generation rate found for the different materials had to vary over order of magnitudes. But in contrast the values listed in tab. 7.6 are approximately equal and independent of the resistivity.

	ρ [Ωcm]		6	100	2000	7000	3000
	$N_{eff,0}$ [cm^{-3}]		$8{\cdot}10^{14}$	$4{\cdot}10^{13}$	$3{\cdot}10^{12}$	$6{\cdot}10^{11}$	$2{\cdot}10^{12}$
Label			933	938	93A	941	MPI
	ΔE_C $[eV]$	σ_n $[cm^2]$	g $[cm^{-1}]$				
E6a	0.39	$1.2{\cdot}10^{-15}$	0.48	0.23	0.29	0.30	0.41
E6b	0.42	$1.0{\cdot}10^{-15}$	0.98	0.54	0.62	0.59	0.71

Table 7.6: Generation rates of E6a and E6b

Therefore it has to be assumed that the E-centre does not contribute to the peak E6 or the contribution is negligible respectively. Since no other peak has been found which could correspond with the E-centre, it has to be concluded that only a very small amount of E-centres is formed.

This conclusion agrees very well with the findings of Su et al. [136], who reported the following ratio to be a constant [7] :

$$\frac{N_{V-O}N_{P,0}}{N_{V-P}N_{O,0}} = 0.07, \tag{7.4}$$

where $N_{P,0}$, $N_{O,0}$ are the initial phosphorus and oxygen concentrations respectively and N_{V-O}, N_{V-P} the concentration of A- and E-centres respectively. Setting $N_{O,0} = 10^{16}$ cm^{-3} and $N_{P,0} = N_{eff,0}$ and replacing the concentration of the A-centre by its generation rate eq. 7.4 can be transformed to estimate the generation rate of the E-centre :

$$g_{V-P} = g_{V-O}\frac{N_{eff,0}}{N_{O,0}}\frac{1}{0.07}. \tag{7.5}$$

For high resistivity material (e.g. $N_{eff,0} = 1{\cdot}10^{12}$ cm^{-3}) the E-centre generation rate is as low as $g_{V-P} = 7{\cdot}10^{-4}$ cm^{-1} and for low resistivity material (e.g. $N_{eff,0} = 1{\cdot}10^{14}$ cm^{-3}) it is $g_{V-P} = 7{\cdot}10^{-2}$ cm^{-1}. Both values are too small to be detected in the big peak E6. Further evidence that the E-centre plays no significant role will be given in the following section.

In contrast to E3 and E6 the fluence dependence of E4 can not be described by one generation rate, which is independent of the doping concentration of the material. In fig. 7.13 it can be seen that the generation rate (n_T/Φ) is higher in material with a higher doping concentration N_{eff}, i.e. the concentration of filled traps n_T increases with N_{eff}. From eqs. 2.36 and 2.41 it follows that the capture process depends on the electron cross section of the defect σ_n and the free electron concentration n, which equals approximately the doping concentration N_{eff} ($r_a \propto \sigma_n n$). The generation rates of the defects correlated with peak E3 and peak E6 do not depend on N_{eff} and therefore it is very likely to assume that the special behaviour rises from the cross section of the single charged divacancy (σ_n(V-V$^-$ $\rightarrow$V-V$^=$)). A small cross section could explain easily the dependence of g_{E4} on the effective doping concentration and it is also in agreement with the assumption considered already in the preceding section, that the electron cross section of a trap-level being negatively charged should be rather small in comparison to the values found e.g. for the A-centre σ_n(V-O^o $\rightarrow$V-O$^-$). Possibly the difference to the value given in tab. 7.4 can be explained by the different methods applied to obtain the results. The indication for a small cross section has been found by observing the capture process, while the higher value was determined from the emission process. Both methods are different in so far, that the determination of the cross section from the emission process requires an extrapolation $1/T \rightarrow 0$, which is unnecessary for the determination from the capture process.

The generation rates extracted from measurements with p$^+$-n -samples are

$$g_{E3} = 1.05{\pm}0.08 \text{ cm}^{-1} \text{ and } g_{E6} = 0.89{\pm}0.04 \text{ cm}^{-1}.$$

The first value is 2.13 times higher and the second 1.33 higher than the results obtained from the other samples. As mentioned above this deviation could arise due to the uncertain extension of the lateral field beyond the central diode. Since

[7] Electron radiation was used, and the concentration of oxygen was varied from $5.5{\cdot}10^{15}$ cm^{-3} to $7.4{\cdot}10^{17}$ cm^{-3}, that of phosphorus from $9.8{\cdot}10^{13}$ cm^{-3} to $2.0{\cdot}10^{16}$ cm^{-3}.

$n_T \propto N_{eff}$ and $N_{eff} \propto A^{-2}$ (see eq. 4.4), the determination of n_T suffers from the inexact knowledge of the effective area. However, comparing N_{eff} as extracted from the depletion voltage (see eq. 2.26) and from the slope (see eq. 4.4) only a factor of 1.25 is found. Thus, if temperature dependent effects are excluded, the uncertainty of the effective area alone does not explain the measured deviation.

7.1.5 Time Dependence and Heat Treatment

Already before the measurements performed 30 days after irradiation, a first measurement on each sample has been made at about 5 days after irradiation, i.e. after room temperature storage for 5 days. It has been found for all samples [8] that peak E3 increased between the first and the second measurement, while peak E6 decreased. Because no change of N_{eff} has been observed in this time range it can be concluded that indeed the trap concentrations changed. In case of peak E3 the increase is about 10 %, and the decrease of peak E6 is about 15 %. For example the change of the peak heights of spectra recorded on 941-samples are shown in fig. 7.14.

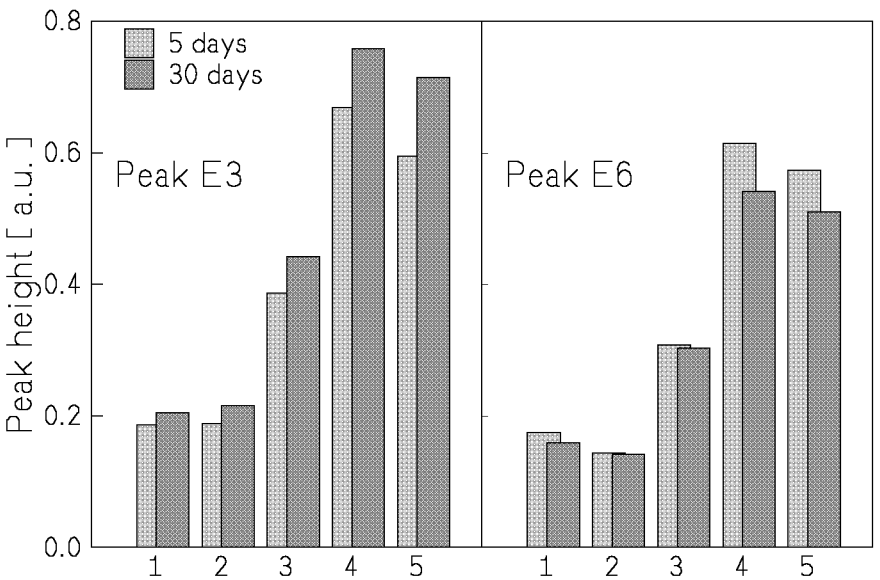

Figure 7.14: Time dependence of peak height. 1 and 2 : $\Phi = 2.88 \cdot 10^{10}$ cm^{-2} (941G06 and -K11), 3 : $\Phi = 5.26 \cdot 10^{10}$ cm^{-2} (941G26), and 4 and 5 : $\Phi = 9.88 \cdot 10^{10}$ cm^{-2} (941G12 and -K13).

The time dependence of the trap concentrations can be expressed in terms of a ratio $n_T(t_2)/n_T(t_1)$ where t_1= 5 days and t_2 = 30 days. In tab. 7.7 the average values of $n_T(t_2)/n_T(t_1)$ as obtained for different materials are summarised. It can be seen clearly that the concentrations of the trap levels E3 and E4 increase, whereas the the concentrations of the trap levels E6a and Eb6 decrease.

[8] except 933-samples which were measured only one time

Besides the parameters determining the energy level of a defect, a further finger print of the defect is its annealing temperature. The E-centre in high resistivity material ($\rho > 50$ Ωcm) anneals out at T <120°C [55], while the divacancy anneals out at a significant higher temperature (see sec. 3.3). Therefore, if again peak E6 is supposed to be a superposition of E-centre and divacancy, it is expected that during an isochronal heat treatment at first the right part of peak E6 decreases and later on (at a higher temperature) the left part.

A p^+-n -sample irradiated with $\Phi = 5.98{\cdot}10^{11}$ cm^{-2} (M20711) has been used to perform the isochronal heat treatment in the temperature range between 353 K and 493 K ($\Delta T = 20$ K, $\Delta t = 20$ min). As can be seen in fig. 7.15 the peak height in total decreased at about 35% after 7 heat treatments. This is in very good agreement with the results obtained by Matheson et al. [137], who found a 25% decrease in γ irradiated silicon (7 heat treatments of 10 min between 370 K and 440 K) and a decrease of about 35% in neutron damaged silicon (14 heat treatments of 10 min between 310 K and 440 K). However, as opposed to the expected behaviour described above it is not the right part (higher temperature) of the peak that diminished, but the left part (lower temperature). The following parameters were obtained applying the analysis of maxima to the remaining peak :

$$\Delta E_C = 0.42 \text{ eV and } \sigma_n = 1.5{\cdot}10^{-15} \text{ cm}^{-2}.$$

Note that these values are the same as found for peak E6b by deconvolution (see tab. 7.6). The concentration n_T was determined to be $3.9{\cdot}10^{11}$ cm^{-3}. Thus also the ratio $n_T/\Phi = 0.65$ cm^{-2} is nearly the same as the value given for the generation rate g_{E6b} in MPI-material (see also tab. 7.6).

Additionally the difference of the peaks measured before and after the 7 heat treatments is shown as a hatched area in fig. 7.15. This 'difference peak' presents the amount of annealed defects. It was possible to apply the analysis of maxima also to this 'difference peak' and the parameters found are :

$$\Delta E_C = 0.39 \text{ eV and } \sigma_n = 1.3{\cdot}10^{-15} \text{ cm}^{-2}.$$

Also in this case the agreement with the values obtained for the peak E6a is convincing. The concentration of annealed defects is $n_T = 3.0{\cdot}10^{11}$ cm^{-3}.

ρ [Ωcm]	100	2000	7000
$N_{eff,0}$ [cm^{-3}]	$4{\cdot}10^{13}$	$3{\cdot}10^{12}$	$6{\cdot}10^{11}$
Label	938	93A	941
	Average Value of $n_T(t_2)/n_T(t_1)$		
E3	1.10	1.14	1.07
E4	1.42	1.16	-
E6a	0.87	0.68	0.81
E6b	0.88	0.76	0.99

Table 7.7: Annealing ratio $n_T(t_2)/n_T(t_1)$ (t_1= 5 d, t_2= 30 d) for irradiation induced trap levels. Ratios smaller than 1 refer to a decrease of the trap concentration in time, ratios greater than 1 to an increase.

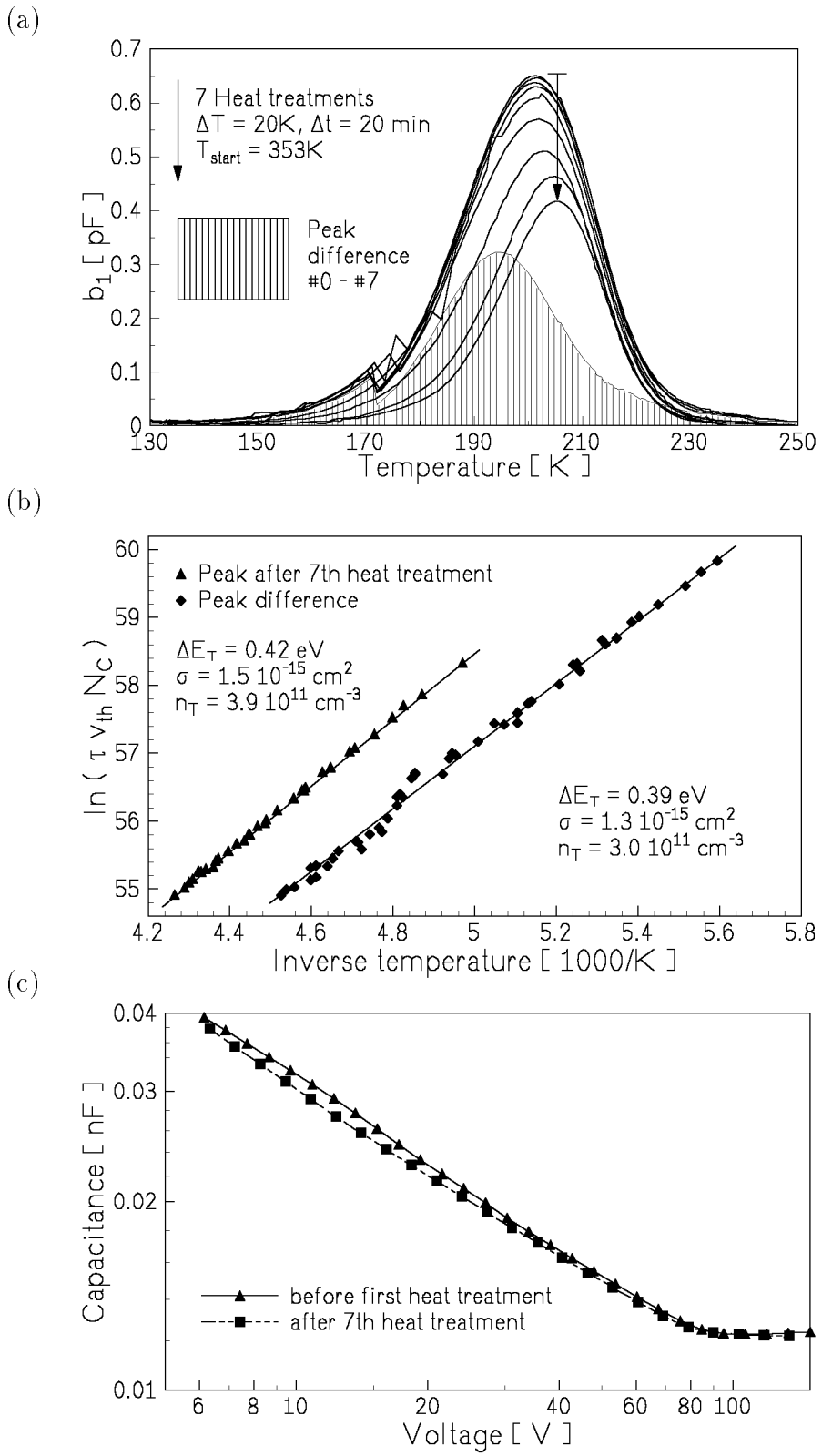

Figure 7.15: Isochronal heat treatment ($\Delta T = 20$K, $\Delta t = 20$ min) of a p^+-n -sample (M20711, $\Phi = 5.98{\cdot}10^{11}$ cm^{-2}). (a) Change of peak E6 due to heat treatments, (b) Arrhenius-plots of remaining peak and 'difference peak', (c) CV-measurements before and after the heat treatments. Note that the depletion voltage did not shift.

Since both energy levels are very similar, it could be concluded from the annealing behaviour that in contrast to the data cited from the literature (e.g. [51]) not E6b should be identified as E-centre, but E6a. But in either cases an annealing of the supposed E-centre should be directly connected with a recovering concentration of donors, which could be easily detected by a change of the depletion voltage. An increase of phosphorus concentration due to the dissociation of the V-P complex (V-P $\rightarrow$ V + P) or its migration to a sink (V-P + X $\rightarrow$ V-X + P) of about $3{\cdot}10^{11}$ cm^{-3} should be seen very clearly as a shift of the depletion voltage of about 15 volts towards higher voltage. But as shown in fig. 7.15 by comparing the CV-characteristics measured before and after the heat treatment the depletion voltage did not change. This is a second strong indication that the E-centre does not contribute to the peak E6.

From the experimental results it can be excluded now that E-centres are responsible for the donor removal : neither the expected dependence on the initial doping concentration of any peak could be observed, nor a recovering of the effective doping concentration correlated with the annealing of a peak. The absence of V-P-complexes can be explained by assuming that the phosphorus is captured in other defect complexes which are not detectable by DLTS. Another possibility to describe the donor removal has been proposed very recently by Matheson et al. [137, 138], who assumed the introduction of only one deep acceptor-level to explain the observed evolution of the effective doping concentration with neutron fluence. However a detailed description of the model has not been published so far.

7.1.6 Hole Traps

In order to determine also parameters of hole traps DLTS-measurements were performed using p$^+$-n -diodes. The hole traps were filled by current injection, i.e. applying a forward bias voltage. The spectrum of electron and hole peaks is shown in fig. 7.16. The electron spectrum consists of 3 peaks E3, E4, and E6, which are already discussed above. In the hole spectrum only one dominant peak is found at about 190 K. The parameters obtained from the analysis of maxima are listed in tab. 7.8.

Sample	Label	ΔE_V $[eV]$	σ_p $[cm^2]$	n_T [cm^{-3}]	g $[cm^{-1}]$	Supposed Identity
p$^+$-n , n-type	H1	0.36	$2{\cdot}10^{-15}$	$1.1{\cdot}10^{11}$	1.1	C_i-O_i
SB, p-type	H1	0.37	$8{\cdot}10^{-15}$	$4.2{\cdot}10^{11}$	1.3	C_i-O_i
	H2	0.54	$4{\cdot}10^{-14}$	$3.4{\cdot}10^{10}$	0.11	unknown

Table 7.8: Parameters of hole traps obtained from a p$^+$-n -sample (M20911, $\Phi = 9.7{\cdot}10^{10}$ cm^{-2}) and a SB-detector (936G15, $\Phi = 3.2{\cdot}10^{11}$ cm^{-2}).

For comparison a DLTS-measurement was performed also for a SB-sample made of p-type material. The main peak (H1) is again found at 190 K, but a second smaller peak (H2) occurs additionally at 250 K, which has not been found in the p$^+$-n -sample. The results obtained from the analysis of maxima are listed in tab. 7.8.

(a)

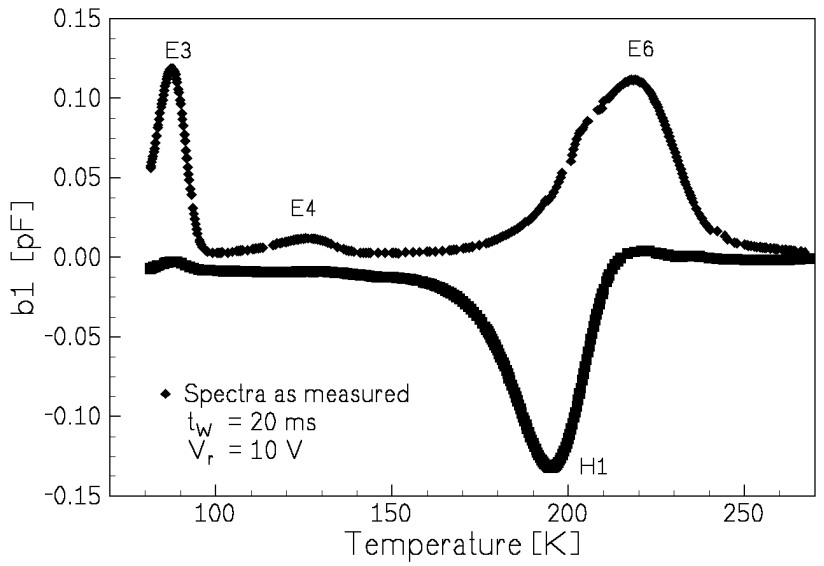

(b)

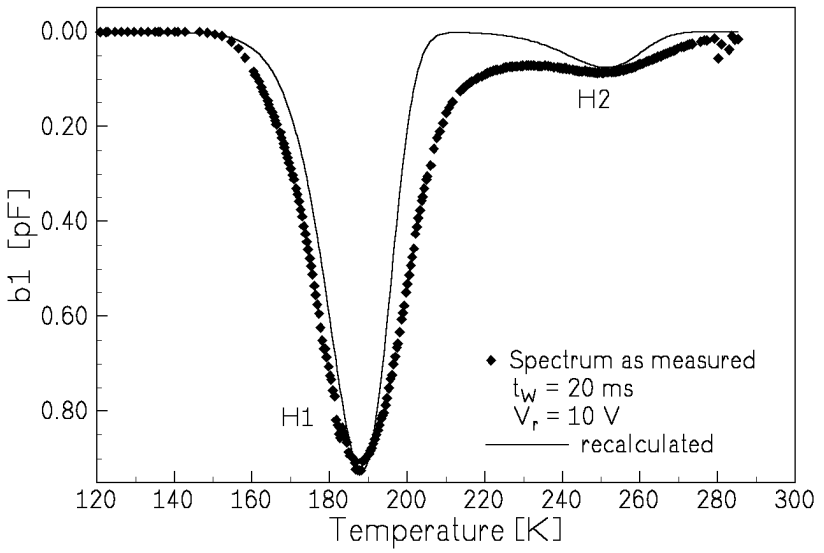

Figure 7.16: (a) : Spectra of p^+-n -sample after irradiation (M20911, $\Phi = 9.47{\cdot}10^{10}$ cm^{-2}). Positive peaks refer to electron traps and negative peaks to hole traps. (b) : Spectrum of p-type sample after irradiation (936G15, $\Phi = 3.2{\cdot}10^{11}$ cm^{-2}). The following parameters were used for the recalculation of the spectrum, H1 : ΔE_V= 0.367 eV, σ_p= $7.6{\cdot}10^{-15}$ cm^2, n_T= $4.16{\cdot}10^{11}$ cm^{-3}, H2 : ΔE_V= 0.538 eV, σ_p= $3.8{\cdot}10^{-14}$ cm^2, n_T= $3.41{\cdot}10^{10}$ cm^{-3}.

For none of both peaks a direct analysis was possible, hence it has to be concluded that similar to peak E6, H1 and H2 are caused by the superposition of several trap levels. This becomes also evident by comparing the measured spectrum with the recalculated one. The parameters found do not describe correctly the measured spectrum (see fig. 7.16). The determined level parameters match very well those of the C_i-O_i-complex.

The introduction rate of the level(s) causing peak is H1 is

$$g_{H1} \approx 1.2 \text{ cm}^{-1}.$$

In contrast to the values obtained for the introduction rates of the electron traps, no significant difference between p^+-n - and SB-samples is found here.

7.2 Thermally Stimulated Current

7.2.1 Introduction

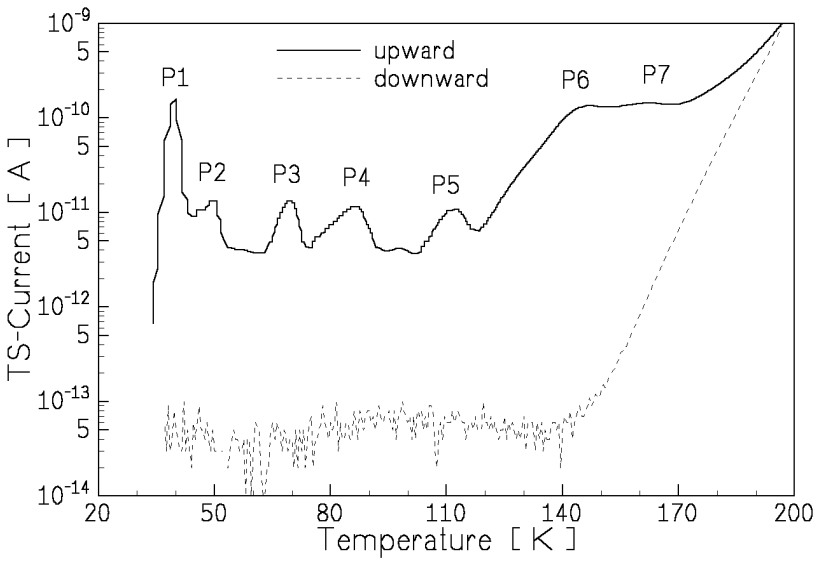

Figure 7.17: Typical TSC-spectrum (Sample : MUEA06, $\Phi = 2.14 \cdot 10^{13}$ cm^{-2}). Note that the current of the corresponding downward measurement is orders of magnitude smaller in the range below 140 K than the TS-current.

Using the technique of TSC for the investigation of radiation induced defects a much greater fluence range can be covered than by DLTS, because the requirement $n_T \ll N_{eff}$ does not apply. However, as will be shown in the following, the high damage level has considerable impact on the determination of the trap concentration. Furthermore remarkable phenomena result from the variation of the trap filling temperature which is different from the temperature of carrier emission, as opposed to DLTS where the temperatures of filling and emission are the same. The main intention of this section is to consider the change of the spectra due to the variation

of the measurement conditions and to discuss the determination of the trap concentration. Therefore the TSC-method was focused on high resistivity material and chiefly on the 0.17 eV level, which allows the demonstration of various phenomena in a rather transparent way.

SB-detectors are not suitable for TSC-measurements, because a proper current injection is not possible. Hence only p^+-n -samples from Micron and MPI were used. Nevertheless two examples of SB-detectors will be presented for demonstration in sec. 7.2.4.

A typical TSC-spectrum is shown in fig. 7.17. In the temperature range between 30 K from 180 K various peaks P1 -P7 are visible. Note that in contrast to DLTS it is not possible to distinguish between hole and electron traps. Above 180 K the TSC-signal is dominated by the current generated in the depleted bulk. In the temperature range below 150 K the current of the corresponding downward measurement is magnitudes of order smaller than the TS-current. The generation current becomes visible in the range above 150 K and grows 4 orders of magnitude within 40 K. With increasing generation current the detection of peaks is hampered by the increase of noise. Thus the temperature range in which the TSC-technique can be applied without restriction is smaller than for DLTS.

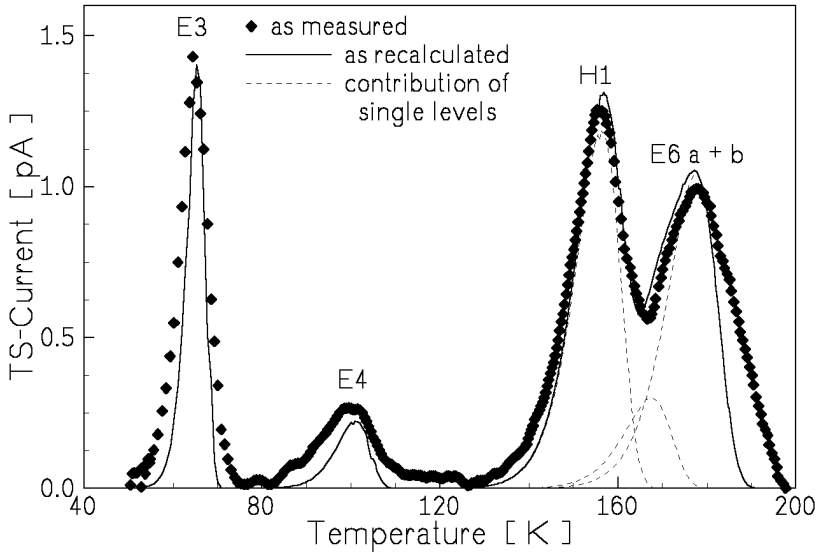

Figure 7.18: Assignment of peaks in the TSC-spectrum (Sample : M20610, $\Phi = 9.51 \cdot 10^{10}$ cm^{-2}) by comparison with DLTS-measurement (see fig. 7.16) : P3 $\hat{=}$ E3, P4 $\hat{=}$ E4, P6 $\hat{=}$ H1, and P7 $\hat{=}$ E6. A level corresponding to peak P5, which can not be seen in this specific spectrum, has not been found by DLTS. The corresponding downward measurement has been subtracted.

Some of the peaks can be assigned to specific defects by comparing the results of a DLTS-measurement with a TSC-spectrum as it is demonstrated in fig. 7.18. The corresponding DLT-spectrum is shown in fig. 7.16a. The energy-level parameters, which were used to recalculate the TSC-spectrum according to eqs. 4.63 and 4.66

are summarised in tab. 7.9. As can be seen in fig. 7.18 the recalculated TSC-signal

Label	ΔE_T $[eV]$	$\sigma_{n,p}$ $[cm^2]$	n_T $[10^{10}$ cm$^{-3}]$
E3	0.17	$1{\cdot}10^{-14}$	1.1
E4	0.25	$1{\cdot}10^{-15}$	0.5
E6a	0.39	$1{\cdot}10^{-15}$	1.5
E6b	0.42	$1{\cdot}10^{-15}$	5.8
H1	0.36	$2{\cdot}10^{-15}$	5.5

Table 7.9: Parameters used for the recalculation of the TSC-spectrum as obtained from DLTS-measurements. Note that the trap concentrations are different due to the uncertainty of the electrodes area and the different sample.

is in good agreement with the measured spectrum. The essential features are reproduced completely. The dominant peak (P3) at 70 K can be associated with the A-centre V-O (E3) and the smaller one (P4) at 100 K corresponds to the double charged divacancy V-V$^{=}$ (E4). The peak structure (P6 and P7) between 140 K and 200 K is caused mainly by the hole trap-level (H1) and the combination of E6a and E6b. One of both corresponds to the single charged divacancy V-V^{-}. In the following those peaks which are identified by comparison with DLTS will be labelled correspondingly as E and H respectively.

However, a comparison with the spectrum shown in fig. 7.17 reveals significant differences concerning the ratio of peak height and the peak resolution, which are caused by the different starting temperature (see sec. 7.2.3) and the different fluences the samples were exposed to. Little differences of the peak temperatures are mainly due to different heating rates.

For demonstration different methods of analysis were applied to peak E3. The results are compared in the next section. The dependence of the TSC-spectra on the starting temperature which is equivalent to the temperature of trap filling and other measurement conditions are discussed in sec. 7.2.3. The fluence dependence of some peaks will be discussed in sec. 7.2.4. In the last section the results of an isothermal heat treatment are presented, which was performed in order to search for a simple correlation of the reverse annealing and the change in one of the defect concentrations.

As expected from the results obtained with the even more sensitive DLTS technique no energy-levels were found in p^{+}-n -samples before irradiation.

7.2.2 Comparison between Different Methods of Analysis

For comparison the different methods of analysis were applied to the A-centre-peak. The results are listed in tab. 7.10. The variation of the heating rate has been not applied because the range of possible variation is too small.

The method of delayed heating is shown very detailed in fig. 7.19. In contrast to the behaviour expected it can be seen from fig. 7.19b that the amount of charge emitted without delay ($t_d = 0$) depends on the temperature. Extrapolating the